Ricerche di Matematica
https://doi.org/10.1007/s11587-022-00691-8

How the nature of behavior change affects the impact of asymptomatic coronavirus transmission

Mohammed H. Alharbi[1] · **Christopher M. Kribs**[2]

Received: 20 April 2021 / Revised: 13 December 2021 / Accepted: 22 March 2022

Abstract
SARS-CoV-2 has caused severe respiratory illnesses and deaths since late 2019 and spreads globally. While asymptomatic cases play a crucial role in transmitting COVID-19, they do not contribute to the observed prevalence, which drives behavior change during the pandemic. This study aims to identify the effect of the proportion of asymptomatic infections on the magnitude of an epidemic under behavior change scenarios by developing a compartmental mathematical model. In this interest, we discuss three different behavior change cases separately: constant behavior change, instantaneous behavior change response to the disease's perceived prevalence, and piecewise constant behavior change response to government policies. Our results imply that the proportion of asymptomatic infections which maximizes the spread of the epidemic depends on the nature of the dominant force driving behavior changes.

Keywords Infectious disease · Mathematical modeling · Asymptomatic cases · Behavior change · COVID-19

Mathematics Subject Classification 92D30 · 91D99

1 Introduction

Beta coronavirus (β-CoV) has caused three severe epidemic outbreaks over the last 20 years (SARS-CoV, MERS-CoV, and COVID-19). β-CoV is one of four genera of coronavirus (CoV), (alpha-, beta-, gamma-, delta-CoV), and divided into four lineages: lineage A (e.g., OC43 and HKU1), lineage B (e.g., SARS-CoV and SARS-CoV-2), lineage C (e.g., MERS-CoV), and lineage D (e.g., HKU9) [1–3]. Coronavirus disease

✉ Mohammed H. Alharbi
mhhalharbi1@uj.edu.sa

[1] Department of Mathematics, College of Science, University of Jeddah, Jeddah, Saudi Arabia

[2] Department of Mathematics, University of Texas at Arlington, Arlington, TX 76019, USA

2019 (COVID-19) is caused by a coronavirus called severe acute respiratory syndrome coronavirus 2 (SARS-CoV-2). It is spread through close contact from one individual to another (within about 6 feet), airborne respiratory droplets (coughs, sneezes, or talks), and aerosol transmission [4].

A serial interval is defined to be the duration from illness onset in a primary case (infector/infective) to illness onset in a secondary case (infectee). An incubation period is defined to be the period between infection and the emergence of symptoms [5, 6]. Recent studies showed that the median serial interval for COVID-19 was estimated at 4.0 days (95% credible interval [CrI]: 3.1, 4.9), and the median incubation period 5.2 days (95% confidence interval [CI], 4.1 to 7.0) [7, 8]. This difference signals that more cases may occur through pre-symptomatic transmission than through symptomatic transmission [7, 9].

Asymptomatic cases are defined as patients who have shown no symptoms for the whole course of the infection. There is mixed evidence on the proportion of asymptomatic cases. Recent studies from Italy and China estimated the proportion of asymptomatic infections at up to 75% and 80%, respectively [10–12]. Other studies have shown a smaller proportion of asymptomatic infections: 41.6% among Japanese nationals evacuated from Wuhan [13], 18% among passengers on the Diamond Princess cruise ship [14], and 10% among children [15]. Several studies have shown that asymptomatic and symptomatic infections have the same relative infectivity [14, 16–18].

Asymptomatic infections are likely to play a significant role in the transmission of COVID-19 for different reasons. First, to predict disease burden when the virus spreads within a population, the proportion of asymptomatic infections is crucial [14]. Second, comprehending how asymptomatic infections contribute to transmission is fundamental to the success of control strategies [19]. In the initial spread of COVID-19, asymptomatic cases can affect the estimated basic reproduction number [20].

Individuals change their behavior during an epidemic, and their behavior has been intricately linked with the spread of infectious diseases historically [21]. Infected individuals may reduce their contact with others due to either illness requiring self-quarantine, isolation upon diagnosis, or government officials' orders to stay home to prevent new cases. Susceptible individuals may take precautionary measures to reduce the number of contact with others to avoid the risk of being infected. Mitigation strategies based on behavior changes, whether individual-based or government-imposed, are (along with contact tracing for limited outbreaks) the primary options available in the early stages of an emerging epidemic. Evidence on behavior changes had strong effects during past pandemics [22–25].

The COVID-19 global pandemic has prompted researchers to analyze and predict its evolution. Mathematical models are a useful tool that can help to predict the epidemic's dynamic and control infectious diseases. A recent systematic review shows that forecasts made by mathematical models are beneficial to understand the pandemic course and guide policy-making [26]. An early study by Wu et al. presented an SEIR meta-population model to simulate the COVID-19 infection across China. They included non-infectious pre-symptomatic cases, but no transmission without symptoms [27]. Another study used the SEIR mathematical model with a quarantine class and governmental intervention measures to mitigate disease transmission. They sug-

gest that governmental intervention strategies can play an essential role in reducing COVID-19 transmission [28].

A recent study by Dobrovolny determined the role of asymptomatic cases in the spread of COVID-19 by using an SAIR mathematical model. Dobrovolny used a different infection rate for asymptomatic individuals determined by a proportionality constant, and a fraction of individuals remain asymptomatic for the whole course of the infection. She concluded that the relative infectiousness of individuals with no symptoms has more impact than asymptomatic proportion on the time course and size of the epidemic [29].

Mathematical models have been used for some time to study the effects of behavior change on the spread of epidemics. In recent decades a substantial literature has developed around the behavioral epidemiology of infectious diseases. A 2010 review by Funk et al. [30] proposed classifying models by (1) whether the information source driving behavior change is globally or only locally available, (2) whether the information source is based on prevalence or on beliefs, and (3) whether the behavior changes individual disease state, parameter values, or contact structure. Later reviews proposed additional classifications, such as whether the behavior change is modeled explicitly or implicitly, i.e., with or without defining a new variable to measure the behavior [31, 32]. Some of the earliest studies used behavior-implicit models in which individuals reduce exposure risk as a function of current infection prevalence (e.g., [33, 34]), which led to sometimes complex dynamics including limit cycles and bistability. Behavior changes which wane with decreasing prevalence can lead to oscillations. Poletti et al. used a behavior-explicit SIR model to investigate spontaneous behavioral change, following cost/benefit considerations, on the spread of an epidemic. Their model accounts for multiple waves and can show asymmetric waves when the behavioral changes and disease dynamics occur on vastly different time scales. They also found that behavioral dynamics results in the reduction of the final attack rate [35]. d'Onofrio, Manfredi and colleagues generalized the basis for exposure-related behavior change to an information index or variable incorporating not only present but past (historical) prevalence levels as well [31, 36, 37]. Buonomo has applied this idea to coronavirus transmission, finding that when the information coverage is high enough, the overall incidence is reduced [38]. Bauch et al. focused review of behavior-explicit models on game-theoretic approaches [31]. A recent systematic review showed that individual-level models are also increasingly used and useful to model behavior changes [39]. For instance, Del Valle et al. used simple and agent-based models incorporating behavioral changes and noted that a second wave of infection can occur when interventions are stopped too soon [40].

In this theoretical study, we consider how varying the proportion of asymptomatic (but equally infectious) cases in an epidemic may affect its size when individuals change their risk behavior, using the current COVID-19 outbreak as a case study. Previous published COVID-19 studies have described at most a single wave of preventive measures to the best of our knowledge. Asymptomatic cases play an essential role in the transmission, but they also do not contribute to the perceived disease prevalence, which drives behavior change during an epidemic. Behavior change can be continuous in response to daily news, or discrete as governments announce policies that last for a month or longer. We seek to identify the theoretical impact of the proportion

of asymptomatic COVID-19 infections on the magnitude of an epidemic under three different behavior change scenarios. To this end, we develop a compartmental model using a nonlinear dynamical system.

2 Model development

We use a modified SEIR model, but with three possible courses of infection: [permanently] asymptomatic, mild symptomatic, and severe symptomatic cases. All of these are assumed equally infectious, but only severe cases are at risk of hospitalization. We distinguish between asymptomatic (infectives who never develop any symptoms) and pre-symptomatic individuals (who will eventually develop symptoms). We consider the case where asymptomatic and symptomatic infections have the same relative infectivity. The constant population size, N, is classified into eight epidemiological classes: susceptible class (S), exposed class (E), pre-symptomatic infectious class (A_P), asymptomatic infectious class (A_L), infective with mild symptoms class (I_M), infective with severe symptoms class (I_S), hospitalized class (H), and recovery class (R, assumed permanent). We also define terms τ and θ to describe the behavior changes (average reduction factors for infectious contact) by individuals with and without (respectively) symptomatic infections. These terms can be taken as constant or time-dependent according to the nature of the behavior change (see more below). The model is described as follows (illustrated in Fig. 1):

$$\begin{cases} \frac{dS}{dt} = \Lambda - \frac{\beta S}{N}\left[\theta(A_L + A_P) + \tau(I_M + I_S)\right] - \mu S, \\ \frac{dE}{dt} = \frac{\beta S}{N}\left[\theta(A_L + A_P) + \tau(I_M + I_S)\right] - (\eta + \mu)E, \\ \frac{dA_L}{dt} = p\eta E - (\gamma_A + \mu)A_L, \\ \frac{dA_P}{dt} = (1-p)\eta E - (\delta + \mu)A_P, \\ \frac{dI_M}{dt} = q\delta A_P - (\gamma_M + \mu)I_M, \\ \frac{dI_S}{dt} = (1-q)\delta A_P - (\epsilon + \mu)I_S, \\ \frac{dH}{dt} = \epsilon I_S - (\gamma_H + \mu)H, \\ \frac{dR}{dt} = \gamma_A A_L + \gamma_M I_M + \gamma_H H - \mu R. \end{cases} \tag{1}$$

Here β is the human-to-human infection rate (modified by τ or θ). η is the rate at which an individual departs the exposed class by becoming infectious (pre-symptomatic, symptomatic, or asymptomatic); p is the proportion of infected individuals who remain asymptomatic for the whole course of the infection. δ^{-1} is the mean time from onset of infectivity to onset of symptoms, for those infectives who eventually develop symptoms; q is the proportion of pre-symptomatic infected who eventually develop mild symptoms. ϵ is the average at which infected with severe symptoms become isolated or hospitalized. γ_A, γ_M, and γ_H are the recovery rates of asymptomatic, infected with mild symptoms, and hospitalized individuals, respectively. To consider how the timespan of a potentially extended outbreak affects the epidemic, we include some demographic effects in the model (not represented in Fig. 1). There is a proportional natural mortality rate μ in each of the eight classes, and Λ

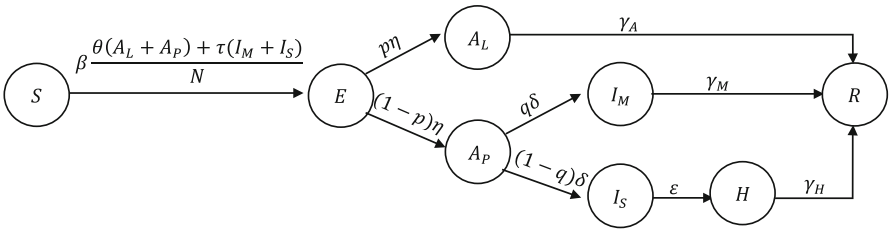

Fig. 1 Flowchart of model (1)

Table 1 State variable and parameter definitions and their units

	Notation	Definition
State variables	$S(t)$	Number of susceptible individuals at time t
	$E(t)$	Number of exposed individuals at time t
	$A_L(t)$	Number of asymptomatic infected individuals who remain asymptomatic for the whole course of infection at time t
	$A_P(t)$	Number of pre-symptomatic infected individuals at time t
	$I_M(t)$	Number of symptomatic infected individuals with mild symptoms at time t
	$I_S(t)$	Number of symptomatic infected individuals with severe symptoms at time t
	$H(t)$	Number of hospitalized infected individuals at time t
	$R(t)$	Number of recovered individuals at time t
Parameters	Λ	Recruitment rate (individual/time)
	μ	Per capita natural mortality rate (1/time)
	β	COVID-19 infection rate (1/time)
	θ	Reduction factor for asymptomatic infection (dimensionless)
	τ	Reduction factor for symptomatic infection (dimensionless)
	p	The proportion of individuals who remain asymptomatic for the whole course of infection (dimensionless)
	q	The proportion of infected with mild symptoms (dimensionless)
	η	1/The duration time from exposure to onset of infectivity (1/time)
	δ	1/The infectiousness period while individuals are pre-symptomatic (1/time)
	ϵ	1/Average hospitalized period for infected with severe symptoms (1/time)
	γ_A	Recovery rate of asymptomatic infected individuals (1/time)
	γ_M	Recovery rate of individuals infected with mild symptoms (1/time)
	γ_H	Recovery rate of hospitalized infected individuals (1/time)

represents the constant inflow of susceptible individuals. Also, in the absence of data on hospital circulation, we assume perfect isolation in the hospital compartment. In this type of model, individuals within the same compartments are considered homogeneous. That is, individuals do not differ based on characteristics such as infectiousness period, behavior changes, age, and or other characteristics. In this model, we consider population-level trends (Table 1).

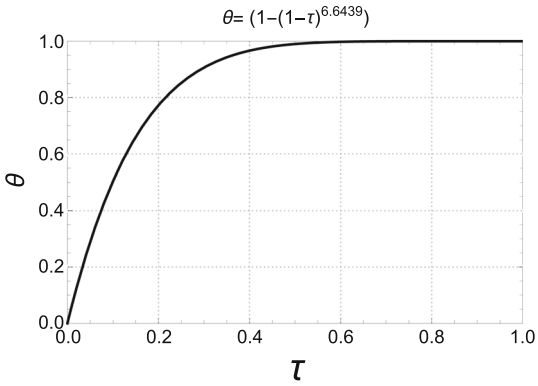

Fig. 2 Relationship between θ and τ

Since there are not any measurements for how asymptomatic and symptomatic cases react while they are infected, we assume that non-symptomatic individuals change their behavior less than symptomatic individuals do: non-symptomatic individuals reduce their potentially infectious contact rate by a factor of θ, while symptomatic individuals reduce it by a factor of τ, with $0 \leq \tau \leq \theta \leq 1$. We consider the two factors connected, $\theta(\tau)$. These factors may remain constant, or may vary over the course of an epidemic, due either to individual reactions to news or to government policies, according to the different scenarios to be considered.

To describe behavior change, we begin by relating θ and τ. First, we assume that non-symptomatic individuals change their behavior less than symptomatic individuals do: non-symptomatic individuals reduce their potentially infectious contact rate by a factor of θ, while symptomatic individuals reduce it by a factor of τ, with $0 \leq \tau \leq \theta \leq 1$. These factors may remain constant, or may vary over the course of an epidemic, due either to individual reactions to news or to government policies, according to the different scenarios to be considered. Second, we fix the relationship between them by considering θ as a function of τ, $\theta(\tau)$, with $\theta(0) = 0, \theta(1) = 1$, and $\theta > \tau$ otherwise. Specifically, we choose an exponential function of the form $\theta(\tau) = 1 - (1 - \tau)^r$ for appropriate r. Third, to derive a value for r, we assume that when symptomatic individuals reduce their contact by 50% ($\tau = 0.5$), asymptomatic individuals only reduce their contact by 1% ($\theta = 0.99$). In this way, only when symptomatic individuals reduce their contact by more than 50%, do asymptomatic individuals reduce their contact significantly. The value of r which fits the (τ, θ) values (0,0), (0.5,0.99) and (1,1) is 6.6439, leading to the relation (shown in Fig. 2):

$$\theta = \left(1 - (1 - \tau)^{6.6439}\right).$$

We consider three different behavior change scenarios in this study. Case one is constant reduction factors, where an environment that is not influenced by the gravity or the magnitude of the epidemic is assumed. It is based on background information that the community has, so it is a constant reduction. This case could represent a scenario where an infection is circulating in other (possibly) nearby communities. Individuals

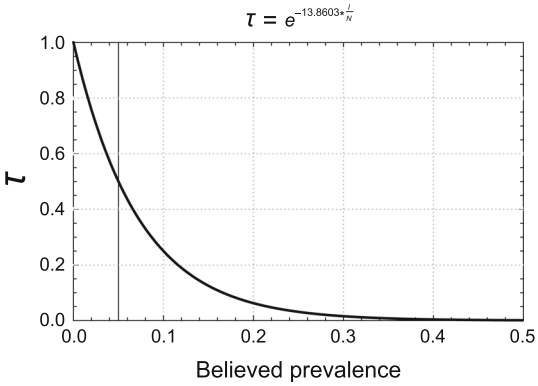

Fig. 3 τ as a function of the believed prevalence

in the study community adapt their behavior in response before the outbreak reaches them, thus constant over time once the outbreak arrives.

Case two assumes reduction factors as a function of the instantaneous prevalence. In this case, we have a completely individual-based or media-based reduction factor, which models the impact of just individuals seeing the news every day and making their decisions. In this case, the symptomatic contact reduction factor (τ) is considered a function of the believed (symptomatic) prevalence I/N, where $I(t) = I_M(t) + I_S(t) + H(t)$. The function $\tau(I/N)$ should be 1 when $I = 0$ and decrease thereafter. Again we choose an exponential function, of the form

$$\tau(t) = e^{k\frac{I(t)}{N(t)}}, \tag{2}$$

where k is the fright parameter describing the intensity of the behavior change. Finally, to fit a value for k, we assume a 50% contact reduction when the perceived prevalence hits 5%, i.e., $\tau = 0.5$ when $I/N = 0.05$. The resulting value is $k = -13.2803$ (see Fig. 3).

Case three uses piecewise constant reduction factors. This case reflects changes by government mandate, which typically do not bounce back and forth instantaneously from one day to another. They tend to be rolled out in phases. In the real world, some asymptomatic cases will be diagnosed, but we assume an environment in which testing is not universal. This model includes the hypothesis of limiting testing availability. Here we assume, for simplification, the government does not know about any of the asymptomatic cases, and policies are made based on the believed prevalence (symptomatic infection prevalence only). The first phase of the outbreak occurs only at the beginning of the infection, where the believed prevalence does not exceed 0.1% (the first threshold). In this phase, there is no reduction in symptomatic infection ($\tau = 1$). The second phase occurs once the believed prevalence exceeds 0.1% (the first threshold). Therefore, a lockdown starts. The government policy is for symptomatic individuals to quarantine completely, but we assume this quarantine (as implemented) is only 95% effective ($\tau = 0.05$). The lockdown remains activated until the believed prevalence rate goes below 0.01% (the second threshold). Thenceforward the lockdown is released gradually, and the believed prevalence rechecked every 30 days. For

Table 2 The behavior change scenarios considered in this study

Case	Cause	Implementation
1	prior knowledge	τ constant
2	spontaneous fear of prevalence	$\tau = e^{-13.2803\, I/N}$
3	government-mandated	initially $\tau = 1$ while $I/N < 0.001$
	lockdown with monthly	then $\tau = 0.05$ until $I/N < 0.0001$
	adjustments	then $\tau = 0.1n$ for 30 days if $I/N < 0.001$ for $30n$ days ($n \leq 10$)

the first 30 days, $\tau = 0.1$, and for the next 30 days (if the believed prevalence does not exceed the first threshold) $\tau = 0.2$, etc. In this manner, the lockdown will continue to be released gradually until the first threshold is reached; thereafter, another lockdown will be activated.

The three cases are summarized in Table 2. In the framework of Funk et al. [30], only case two qualifies as a BEID model, since behavior is considered constant in case one, and imposed by governmental constraints rather than spontaneous individual decisions in case three. However, note that in both cases two and three, $\tau(t)$ provides an explicit, time-varying description of average risk behavior coupled to infection. The information source, perceived (symptomatic) prevalence, is assumed globally known.

When new, behavior-related variables describe the result of the behavior, a model is considered phenomenological. When those variables describe the process of making a decision (often discrete, typically binary), it is termed mechanistic. In this regard, the models in this study, like others which describe the collective effects of such decisions using information indices, are phenomenological.

3 Analysis

The control reproduction number, $\mathcal{R}_c$, is one of the most significant thresholds, which measures the infection's ability to spread. We use $\mathcal{R}_c$ instead of using the basic reproduction number, $\mathcal{R}_0$, because we incorporate control measures (τ and θ) in the model. Although reproduction numbers are defined for outbreak models with no demographics, the next-generation approach we apply is not, as it requires a non-isolated disease-free equilibrium. We, therefore, retain recruitment (Λ) and natural mortality (μ) for our analytical work because they are necessary to avoid having infinitely many non-isolated disease-free equilibria. They can then be set to zero if desired when calculating numerical values for $\mathcal{R}_c$. For case two and three, in which behavior change only starts after the outbreak reaches a certain level, the initial values of θ and τ are taken to be one, which simplifies $\mathcal{R}_c$ to $\mathcal{R}_0$.

The point where no disease is present in the population (the DFE) occurs for model (1) when $A_L = A_P = I_M = I_S = 0$. Setting all differential equations in (1) equal to zero, we find the DFE of the form $(\frac{\Lambda}{\mu}, 0, 0, 0, 0, 0, 0, 0)$.

To drive the $\mathcal{R}_c$ for model (1), we use the next-generation operator method proposed by Diekmann and Heesterbeek [41]. We begin with separating the model's classes into

uninfected (X), noninfectious infected (Y), and infectious (Z) classes;

$$X = \begin{pmatrix} S \\ R \end{pmatrix}, \; Y = \begin{pmatrix} E \\ H \end{pmatrix}, \; Z = \begin{pmatrix} A_L \\ A_P \\ I_M \\ I_S \end{pmatrix}.$$

After substituting the equilibrium values of the noninfectious infected classes (Y) into the differential equations for the infectious (Z) classes, we compute the Jacobian matrix

$$A = \frac{\partial}{\partial Z}\left(\frac{\partial Z}{\partial t}\right).$$

Computing A at the DFE for model (1), we obtain A= M - D, with

$$M = \begin{pmatrix} \frac{\beta\eta\theta p}{\eta+\mu} & \frac{\beta\eta\theta p}{\eta+\mu} & \frac{\beta\eta p\tau}{\eta+\mu} & \frac{\beta\eta p\tau}{\eta+\mu} \\ \frac{\beta\eta\theta(1-p)}{\eta+\mu} & \frac{\beta\eta\theta(1-p)}{\eta+\mu} & \frac{\beta\eta(1-p)\tau}{\eta+\mu} & \frac{\beta\eta(1-p)\tau}{\eta+\mu} \\ 0 & \delta q & 0 & 0 \\ 0 & \delta(1-q) & 0 & 0 \end{pmatrix},$$

and

$$D = \begin{pmatrix} \gamma_A + \mu & 0 & 0 & 0 \\ 0 & \delta + \mu & 0 & 0 \\ 0 & 0 & \gamma_S + \mu & 0 \\ 0 & 0 & 0 & \epsilon + \mu \end{pmatrix}.$$

The control reproduction number $\mathcal{R}_c$ is obtained as the spectral radius of $M \cdot D^{-1}$, precisely,

$$\mathcal{R}_c = \frac{1}{2}\left(a + \sqrt{a^2 + 4b}\right), \tag{3}$$

where

$$a = \frac{\beta\eta\theta p}{(\eta+\mu)(\gamma_a+\mu)} + \frac{\beta\eta\theta(1-p)}{(\delta+\mu)(\eta+\mu)},$$
$$b = \frac{\beta\delta\eta(1-p)q\tau}{(\delta+\mu)(\eta+\mu)(\mu+\gamma_s)} + \frac{\beta\delta\eta(1-p)(1-q)\tau}{(\delta+\mu)(\eta+\mu)(\mu+\epsilon)}.$$

The first term of a refers to the contribution of asymptomatic individuals, who remain asymptomatic for the whole course of the infection, while the second term of a refers to pre-symptomatic infection. Furthermore, the first and second terms of b refer to the contribution to infection by individuals with mild and severe symptoms. Numerical simulation will be performed on $\mathcal{R}_c$ in the next section using estimated parameter values.

Table 3 Summary of estimated model parameters

Par. (unit)	Value	Range
Λ (individual/day)	0	–
μ (days^{-1})	0	–
β (days^{-1})	0.399322	0.299216–0.530679
η (days^{-1})	0.668558	0.641876–0.822624
δ (days^{-1})	0.269961	0.183754–0.346695
q (dimensionless)	0.8 [42, 43]	–
ϵ (days^{-1})	1/10 [44]	–
γ_A (days^{-1})	1/7	1/9 – 1/6
γ_M (days^{-1})	1/21	–
γ_H (days^{-1})	1/14	–

4 Numerical simulation

We find parameter values either from previous literature or by estimation. We consider three different behavior change cases, τ, in this section-the first case when τ is constant over time, the second case when τ is continuously changing over time, and the third case when τ is piecewise constant changing over time.

4.1 Parameter estimates

Some parameter values were obtained directly from previously published studies, as listed in Table 3, while the others were estimated in this study.

The average time to recovery ranged from seven to 32 days for mild cases and 21 to 32 days for severe cases [43, 45–48]. We pick seven days as the recovery time for asymptomatic cases ($\gamma_A = 1/7$), 21 days for mild cases ($\gamma_M = 1/21$), and 24 days for severe cases. After applying the average isolation days for severe cases ($\epsilon = 1/10$), we get $\gamma_H = 1/14$.

To estimate the remaining parameters in this model (β, η, and δ), we use the average reported basic reproduction number (averaged from published estimates of $\mathcal{R}_0$ is 3.28 [49]), serial interval (estimated at 4.0 days [7]), and incubation period (estimated at 5.2 days [8]) for COVID-19. Then, we use a two-part process: first linking these parameters to each other, then using a back-estimation approach to calculate those parameters. The serial interval is the average waiting time before the first infection happens ($1/\beta$), adding to the average duration time from exposure to infectivity onset ($1/\eta$). The incubation period is $1/\eta$, adding to the infectiousness period, while individuals are pre-symptomatic ($1/\delta$). Therefore, we use the relation $\frac{1}{\eta} + \frac{1}{\beta} = 4$ and $\frac{1}{\eta} + \frac{1}{\delta} = 5.2$ to obtain β and δ as functions of η. This made (3) an equation to a function of η alone (with $\tau = \theta = 1$). This allows us to obtain estimates for η, β and δ. All the parameter estimates are summarized in Table 3.

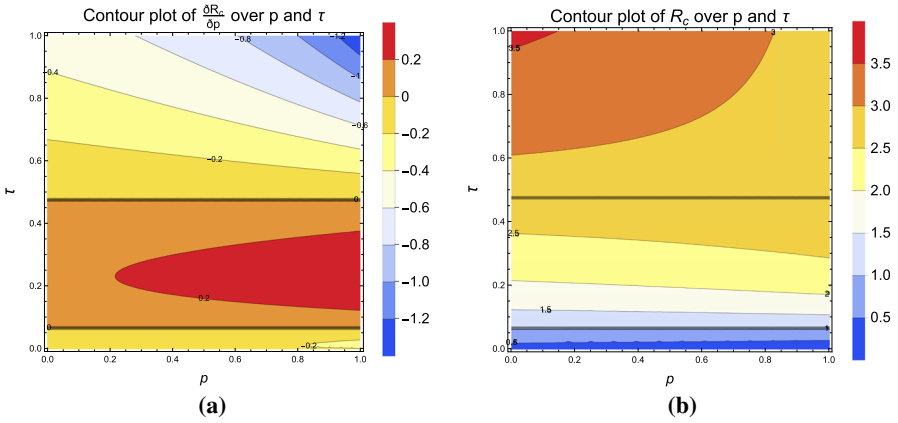

Fig. 4 Contour plot of CRN over p and τ

4.2 Case one: constant reduction in contact factors

When behavior change is constant, independent of the course of the epidemic, $\mathcal{R}_c$ provides one measure of its initial growth. We, therefore, consider how $\mathcal{R}_c$ is affected by the proportion of asymptomatic infections (p), in conjunction with the magnitude of behavior change as represented by τ. By substituting parameter values from table 2 into CRN and considering τ and p to be constants that vary between zero and one, contour plots of $\frac{\partial \mathcal{R}_c}{\partial p}$ and $\mathcal{R}_c$ over p and τ were generated, Fig. 4a and b, respectively.

Figure 4a shows the contour plot of the partial derivative of $\mathcal{R}_c$ with respect to p as τ and p vary. In this figure, there are three regions. Region one, when τ is between 0.5 and one, shows that as p increases, $\frac{\partial \mathcal{R}_c}{\partial p}$ decreases with negative slopes. Region two, when τ is between 0.05 and 0.5, indicates that $\frac{\partial \mathcal{R}_c}{\partial p}$ goes up as p goes up with positive slopes. Lastly, region three, when τ is between 0 and 0.05, depicts the same behavior as region one.

Figure 4b shows the contour plot of $\mathcal{R}_c$ over p and τ. By applying the three regions from Fig. 4a, we get the top region where symptomatic individuals do not reduce their contacts by more than 50%, and almost no behavior change in individuals with no symptoms (i.e., $\tau \in (0.5,1)$, $\theta \in (0.99,1)$). In this region, we notice that $\mathcal{R}_c$ is the highest when $p = 0$. Plus, as p increases, $\mathcal{R}_c$ decreases. In this connection, symptomatic individuals are contributing more to the initial spread of the disease than asymptomatic individuals.

In the next region, region two, as in reality, when people aware of the outbreak, symptomatic individuals will be isolated more since initial recommendations were that people who have symptoms should isolate themselves. In this matter, symptomatic individuals are reducing their contacts more than 50%, while individuals with no symptoms are reducing their contacts, but less than individuals with symptoms ($\tau \in (0.05,0.5)$ and $\theta \in (0.3,1)$). In this region, we discern that as p increases, $\mathcal{R}_c$ increases. Thus, asymptomatic individuals are contributing more to the initial spread of the

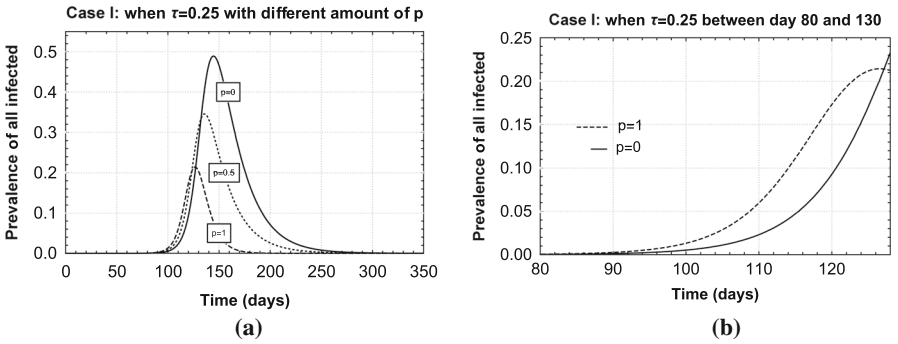

Fig. 5 Height of prevalence with different amount of p when $\tau = 0.25$ for case one

disease than symptomatic individuals. Further, symptomatic individuals are reducing their contacts by a higher factor than their ability to spread the disease better.

In region three, individuals with symptoms are reducing their contacts by more than 95%, while asymptomatic individuals are reducing their contacts by more than 70% ($\tau \in (0,0.05)$ and $\theta \in (0,0.3)$). In this setting, as p increases, $\mathcal{R}_c$ decreases. Further, symptomatic individuals are contributing more than individuals with no symptoms.

We also perform numerical simulations of the model to see how the entire course of the epidemic varies depending on p and τ, using our best estimates of the parameter values. We computed the number of active cases throughout the outbreak, for different values of p and τ. Figure 5 illustrates the range of results over time for all values of p, for $\tau = 0.25$, a representative value from region two in which symptomatic individuals reduce their contact rate by a factor of four.

We have a couple of results that may appear to contradict the control reproduction number (CRN). One is that the height of the peak of prevalence decreases with p (especially, if $\tau \in$ region 2 see Fig. 5a). Further, the fraction of individuals who never get infected increases with p for all values of τ (see Fig. 5b when $\tau \in$ region 2). These results seem to contradict the contour plot of the CRN and what has been said about the three regions (see Fig. 4b). However, the CRN describes the rate of spread of disease at the edge of an outbreak. Figure 5a is representing the peak of an epidemic, which is far away from the boundary of the epidemic. Namely, the CRN is not a good measure of how well the disease spreads when there are many infected individuals. In addition to that, the fraction of asymptomatic individuals is more significant away from the edge of the epidemic. Thus, the CRN tells about the spread of the disease at the beginning of the outbreak. The peak of prevalence and the final fraction of susceptibles depend on events far away from the beginning of the epidemic. So, they do not necessarily follow the same pattern as the CRN.

Therefore, there are multiple possible measures by which we may take an optimum value of p. By saying an optimum value of p, we refer (implicitly) to the evolutionary perspective of the pathogen. Hence, the optimum value of p means the most infection possible, which is chosen to maximize the CRN, maximize the peak of prevalence, and minimize the fraction of susceptibles at the final time. Consequently, the value of p that maximizes CRN is zero for τ in regions one and three and one for τ in

region two. However, to maximize the height of prevalence and minimize the fraction of susceptibles at the final time, p should be zero for all values of τ.

Hence, most pathogen success measures are maximized when p is zero, which implies that there are no asymptomatic infections, except when τ in region two. When τ is in region two, $p = 1$ maximizes only the outbreak's initial spread since asymptomatic infections remain less infectious than symptomatic infections.

4.3 Case two: continuous infection reducing factors as a function of the prevalence

Figure 6a indicates the prevalence over time of all infected with varying proportions of asymptomatic infections (p) between zero and one. The height of the peak of the prevalence increases for p between 0 and 0.59, and then it decreases for higher p. For lower p, we notice that the epidemic's shape is asymmetric because most of the cases are observed. Moreover, for high values of p, most of the cases are unobserved and, therefore, there is not much behavior change; consequently, we see the shape of the epidemic is symmetric. The optimum value, $p = 0.59$, maximizes the highest peak of the epidemic since behavior changes react to less than half of the infections. In contrast, when $p = 0$, behavior changes work at the best capacity. Lastly, when $p = 1$, there are no behavior changes.

Figure 6b illustrates the fraction of susceptibles, who never get infected, at the final time with varying p between zero and one. The lower curve depicts the case with no behavior change, which is similar to case one. The upper curve shows the case two with behavior changes. In this case, the final fraction of susceptibles increases for p between zero and 0.52, but then it turns around and gets low for higher p until it reaches the lowest point at $p = 0.885$. For p between 0 and 0.52, behavior changes work well with the gradual increases of p to minimize the final fraction of susceptibles. On the other hand, when p is between 0.52 and 0.885, more than half of the infection is unobserved, indicating fewer behavior changes. For $p > 0.885$, most of the infection is asymptomatic, so the final fraction of susceptibles is approaching to match the case with no behavior change. From the pathogen's evolutionary perspective, the lower the uninfected fraction at the final time, the stronger the outbreak was.

Unlike case one, we notice in case two that a higher peak does not necessarily mean the worst outbreak, i.e., the height of the prevalence peaks when $p = 0.59$ whereas the lowest fraction of susceptibles is when $p = 0.885$. Behavior change reduces the infection more when p is low since the symptomatic prevalence represents most of the infections. The entire course of the epidemic produces the highest peak with the smallest overall outbreak for p between 0.52 and 0.59. For $p = 0.885$, the epidemic displays a relatively lower peak but with the largest overall outbreak. For $p = 1$, the epidemic exhibits both the lowest peak and the smallest overall outbreak.

4.4 Case three: piecewise constant reduction in contact factors

In this case, we model the changes by government mandate policies. Numerical simulations of the case three model are performed. We compute the total infection prevalence

with different amounts of the proportion of asymptomatic infection (p) and the behavior changes ($\tau(t)$) by government mandate policies.

Figure 7a indicates the total infection prevalence changes over time due to government policies (the lockdown). Regardless of the proportion of asymptomatic infected (only if $p < 1$), the government policies invoked during a lockdown produce enough behavior change ($\tau(t)$) to pull down the total infections to the second threshold. When $p = 0$, which means all infected individuals are symptomatic, government intervention policies are well designed to the perceived prevalence. For $p > 0.5$, the policies are implemented in response to half or less of the total infections. For higher p, since perceived prevalence takes a longer time to reach the first threshold, government policies take a longer time to be implemented. A higher value of p makes the initial peak higher and later than the lower value of p because the government does not perceive the asymptomatic infections. Also, a higher value of p means the epidemic takes longer to spread. However, the duration between waves is shorter when p is high because the asymptomatic infections do not last as long as symptomatic ones. Furthermore, any effective government policies prolong the outbreak for at least five years (if $p \leq 0.75$), during which time there will continue to be regular peaks. Through the

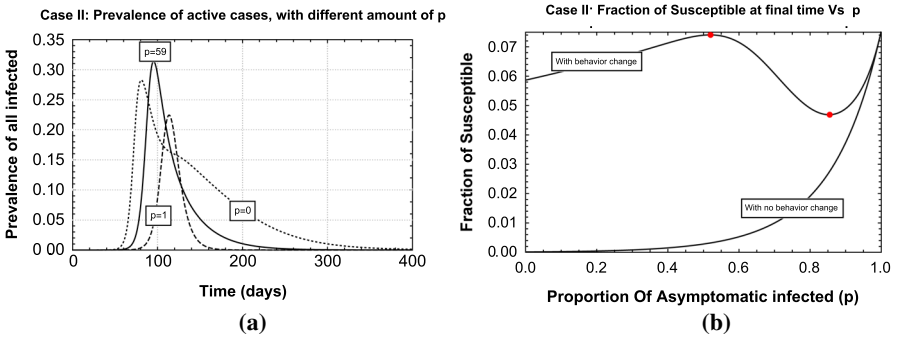

Fig. 6 Height of prevalence and fraction of susceptibles at final time with different amount of p when τ varies over time with the perceived prevalence

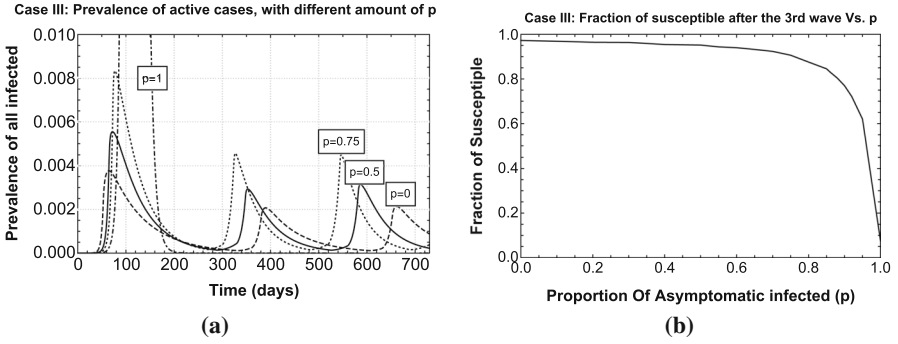

Fig. 7 Height of prevalence and fraction of susceptibles at final time with different amount of p when τ piecewise constant varies over time

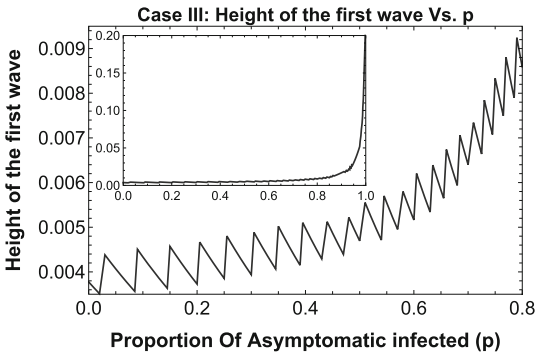

Fig. 8 The peak of the first wave as a function of the proportion of asymptomatic infections (for $0 \leq p \leq 0.8$)

first five years, the peak of each wave is not diminishing. This isolation behavior will continue for a long enough time scale that demographics will start to be significant. For $0.99 < p < 0.997$, there are at most two phases of government lockdown, while for $p > 0.9977$, hardly any symptomatic infections are noticed, and therefore no government policy is implemented.

Figure 7b shows the fraction of susceptibles, after the third wave of the infection, with varying p between zero and one. In contrast to cases one and two, the fraction of susceptibles decreases with p since the behavior change reacts less with more asymptomatic infections. For p between zero and 0.75, the fraction of susceptibles decreases slowly to reach 0.9 due to behavior changes, which indicates that only less than 10% of individuals have been infected. Meanwhile, if $0.75 < p < 0.95$, the fraction of susceptibles decreases from 0.9 to 0.6 since the behavior changes only respond to less than 25% of the total infection. For $p > 0.9977$, there is no behavior change, and the final fraction of susceptibles is approaching the case with no behavior change.

We further compute the highest point of the first wave's prevalence as a function of the proportion of asymptomatic infections (p). Figure 8 shows that the general trend of the peak is going up with p. However, as p increases in a tiny amount, the peak goes up and down, not in a monotone way because of the discretization of the lockdown's starting day. The lockdown day is not the exact instant of passing the first threshold; it is at the next integer value day after. Moreover, as p increases in a tiny amount, the increased proportion of asymptomatic cases reduces the first wave's peak, making the graph go down until the point where the government policy is implemented a day later causing the sudden jump. The peak prevalence decreases gradually with small increases in p because the asymptomatic infections spread the virus less than symptomatic infections. However, at some point, the decrease in perceived prevalence postpones the onset of behavior changes by a day, causing an abrupt jump in Fig. 8. Therefore, the time elapsed between the instant in time when it passed the first threshold and the next day when the census is taken varies as p varies in tiny amounts.

When the proportion of asymptomatic infections (p) is low, the epidemic spreads faster. This implies that the control measures are implemented relatively soon, and the epidemic peak is relatively low. Then, as p increases, the epidemic spreads more slowly initially, since asymptomatic infections spread it less. Besides, since fewer

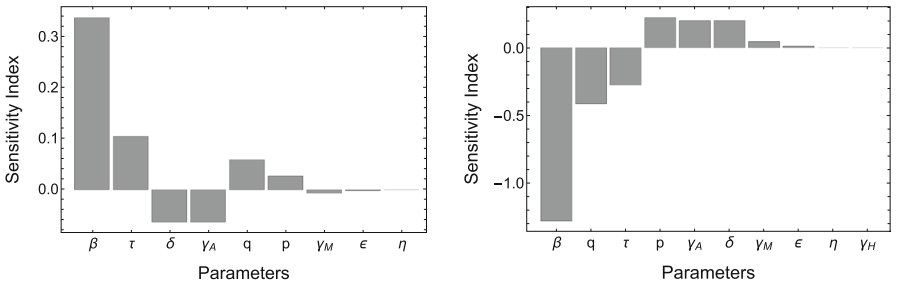

Fig. 9 Sensitivity analysis for $\mathcal{R}_c$ (**a**) and S_{tf}^* (**b**): Sensitivity indices are listed in order of decreasing magnitude

cases are observed, the lockdown starts even later, which indicates that the peak is more heightened. Further, when p is high enough, there will never be enough perceived cases to initiate the lockdown, and the epidemic matches the case with no behavior changes.

Although not shown here, we obtained qualitatively identical results for the dependence of symptomatic prevalence and severe cases on p.

4.5 Sensitivity and uncertainty analysis

The goal of this subsection is to verify that our qualitative results are independent of the parameter values. We performed a sensitivity analysis of the CRN (Fig. 9a) and the fraction of susceptibles at final time (S_{tf}^*) (Fig. 9b) to determine how variations in parameter values impact $\mathcal{R}_c$ and S_{tf}^*. Namely, we increase each parameter by 0.1% (while preserving other parameters at the baseline values obtained in Table 3) and calculate the normalized sensitivity index. The results of the sensitivity analysis shown in Fig. 9 indicate the CRN is most sensitive to the infection rate (β), the reduction factor for symptomatic infection (τ), 1/the infectious period while individuals are pre-symptomatic (δ), the recovery rate of asymptomatic infected individuals (γ_A), and the proportion of infected with mild symptoms (q). S_{tf}^* is also influenced by β, q, τ, the proportion of individuals who remain asymptomatic for the whole course of infection (p), γ_A, and δ. Remarkably, both measures (CRN and S_{tf}^*) are highly sensitive to τ and p, which are scrutinized in this study. Among the parameters with higher sensitivity indices to both (CRN and S_{tf}^*), the proportion of infected with mild symptoms (q) is well-known [42, 43, 50].

Using ranges for the serial interval, incubation period, and basic reproductive number and the same method as Sect. 4.1, we can estimate the ranges of parameter values (shown in Table 3). Figure 10 indicates the S_{tf}^* for case one (at the bottom of the figure) and case two (at the top of the figure) with δ over its range. The qualitative results for all three cases remain the same, which shows that our results are not dependent on parameter estimates. Hence, our qualitative results are robust and independent of parameter values.

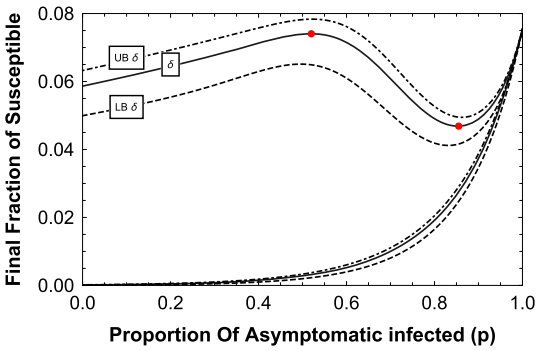

Fig. 10 S_{tf}^{*} for case one (bottom) and case two (top) with δ over its range: dashed lines indicate the lower bound for δ; dot-dashed lines indicate the upper bound for δ; solid lines indicate the baseline value for δ

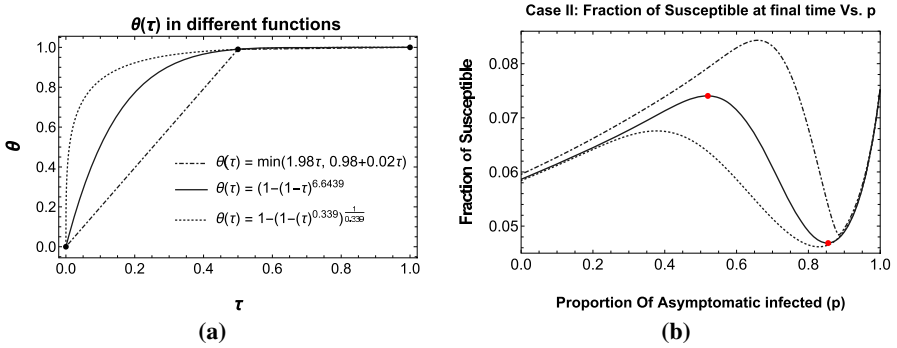

Fig. 11 **a** Different functions represent the relationship between θ and τ; **b** S_{tf}^{*} for case two with different functions of $\theta(\tau)$

Figure 11a indicates three different functions representing the assumed relationship between θ and τ. Indeed, the two new functions work as extreme cases. One is a less reactive change where asymptomatic individuals only change their behavior when symptomatic individuals are already nearly wholly isolated, while the other is the least reactive convex function possible. Figure 11b shows S_{tf}^{*} with the different $\theta(\tau)$ functions shown in Fig. 11a. The dot-dashed curve in Fig. 11b (represented by the piecewise linear function (dot-dashed line in Fig. 11a) shows that the more asymptomatic individuals change their behavior relative to symptomatic individuals ($\theta(\tau)$), the more complex the dependence on p for the size of the epidemic—specifically, the more pronounced the non-monotone variation is for the epidemic size. All three functions describing the behavior change of asymptomatic individuals yield the same type of dependence of S_{tf}^{*} on p, showing that our qualitative results are robust.

5 Conclusion

We analyzed a deterministic compartmental model to evaluate and predict the impact of the proportion of asymptomatic infections (p) under three different behavior change scenarios finding that p plays a large role in changing the size and the time of the

epidemic. Although the model is still too simplistic in directly guiding policymakers to mitigate the effects of p, and it is not intended to do so, the qualitative trends predicted by our simulations can be beneficial in designing studies to quantify the influence of these asymptomatic infections. Our parameter estimates suggest that symptomatic infections spread the disease more than asymptomatic ones because the infectious period lasts longer, even considering effective isolation following diagnosis.

If behavior change is considered constant, which may occur based on background information that a community has, then the epidemic size is maximized, and the final fraction of susceptibles is minimized, when p is low. On the other hand, a high value of p maximizes only the outbreak's initial spread when the behavior change (τ) ranges between 0.05 and 0.5.

If, instead, behavior change occurs due to an instantaneous response to the disease's perceived prevalence, then the highest peak with the smallest overall outbreak occurs when p is between 0.52 and 0.59. Further, the epidemic reveals a relatively lower peak but with the largest overall outbreak when $p = 0.885$. The lowest peak with the smallest epidemic is shown when $p = 1$.

Finally, if behavior change occurs in response to government policies, then a higher value of p plays a significant role in changing the epidemic's duration, and maximizes the epidemic size. In contrast, a lower value of p means a significant behavior change is implemented since most of the infected individuals are observed. Therefore, the epidemic shows both the lowest peak and the smallest overall outbreak.

If p is high, that maximizes the epidemic size and plays a significant role in changing the epidemic's duration under scenario case three. Furthermore, a higher value of p contributes only to the infection's initial spread of the disease if the behavior change (τ) remains constant and ranges between 0.05 and 0.5. Moreover, if the behavior change is considered changing continually as in case two, then a higher value of p minimizes the disease's initial spread and the epidemic size.

A lower value of p maximizes the epidemic size if the behavior change (τ) is a constant (case one). Suppose τ is considered to be as in case two and three. In that case, a lower value of p means a significant behavior change is implemented since most of the infected individuals are observed. Therefore, the epidemic shows both the lowest peak and the smallest overall outbreak.

Intermediate values of p, which are essential only under instantaneous behavior change, produce the highest peak and minimize the epidemic size.

In reality, behavior change occurs through all three of these mechanisms. There is a priori information. There are instantaneous behavior changes when individuals make their own decisions. There are also behavior changes that individuals may make when mandated by government policies. In this study, we have seen the effects of each of those forces separately. As the COVID-19 pandemic has spread across the world, we have seen government policies and individuals' behavior vary significantly from one country to another and from one state to another within the United States. It is essential to understand that the pandemic will play out differently depending on the dominant force behind people's behavior change.

In [35], the authors used a time scale argument and asymptotic expansion to show when the spontaneous behavioral changes and diseases dynamics occur on vastly different time scales, then their model observes multiple epidemic waves. In our model,

delays in behavior change are necessary to show many waves within the same outbreak and asymmetric shapes of the epidemic, i.e., rising and decaying phases of the epidemic are different in shape, similar to [35]. Further, the present study model shows that the final fraction of susceptibles varies as p varies with significant behavior change. Our results are consistent with [40] that the second wave of infection, in case three, can occur when interventions are stopped too soon. Note that in [38], Buonomo's vaccination rate is composed of a constant part, like our case one model, plus a prevalence-dependent part, similar to our case two model but with memory.

One of the limitations of this study is that we have assumed a consistent government policy. However, we have seen in the United States and some other countries that there are multiple waves, but they differ. The second wave is higher than the first one because the government policies have been changing throughout the outbreak. Government policies have been inconsistent, making the shape of the pandemic irregular. Another limitation is that little to nothing was known about the characteristics of SARS-CoV-2 at the beginning of the current outbreak, which has produced a great variety of estimates about the disease's epidemiological characteristics as recovery time and proportion of asymptomatic infections. This limits the quantitative accuracy of our predictions, but the qualitative results hold even for other parameter values. In the future, we hope to extend our model to include two different diseases under different behavior change scenarios. Varying the relative infectiousness between asymptomatic and symptomatic infection is also a potential extension of this study. An Agent-Based Model (ABM) can be developed to allow such variations in individuals in epidemiological characteristics and behavioral. Further, models like our case two model can be extended to include a degree of memory using such an information index.

References

1. Weiss, S.R., Navas-Martin, S.: Coronavirus pathogenesis and the emerging pathogen severe acute respiratory syndrome coronavirus. Microbiol. Mol. Biol. Rev. **69**(4), 635–664 (2005)
2. Su, S., Wong, G., Shi, W., Liu, J., Lai, A.C.K., Zhou, J., Liu, W., Bi, Y., Gao, G.F.: Epidemiology, genetic recombination, and pathogenesis of coronaviruses. Trends Microbiol. **24**(6), 490–502 (2016)
3. Yang, Y., Peng, F., Wang, R., Guan, K., Jiang, T., Guogang, X., Sun, J., Chang, C., The deadly coronaviruses: The, : SARS pandemic and the 2020 novel coronavirus epidemic in China. J. Autoimmunity **102434**, 2020 (2003)
4. Centers for Disease Control and Prevention. Coronavirus Disease 2019 (COVID-19). https://www.cdc.gov/coronavirus/2019-ncov/prevent-getting-sick/how-covid-spreads.html. Access date: September (2020)
5. Fine, P.E.M.: The interval between successive cases of an infectious disease. Am. J. Epidemiol. **158**(11), 1039–1047 (2003)
6. Svensson, Å.: A note on generation times in epidemic models. Math. Biosci. **208**(1), 300–311 (2007)
7. Nishiura, H., Linton, N.M., Akhmetzhanov, A.R.: Serial interval of novel coronavirus (COVID-19) infections. Int. J. Infect. Dis. **93**, 284–286 (2020)
8. Li, Q., Guan, X., Wu, P., Wang, X., Zhou, L., Tong, Y., Ren, R., Leung, K.S.M., Lau, E.H.Y., Wong, J.Y., et al.: Early transmission dynamics in Wuhan, China, of novel coronavirus–infected pneumonia. N. Engl. J. Med. **382**, 1199–1207 (2020)
9. Ferretti, L.., Wymant, C., Kendall, M., Zhao, L., Nurtay, A., Abeler-Dörner, L., Parker, M., Bonsall, D., Fraser, C.: Quantifying SARS-CoV-2 transmission suggests epidemic control with digital contact tracing. Science, **368**(6491), (2020)

10. Day, M.: Covid-19: identifying and isolating asymptomatic people helped eliminate virus in italian village. BMJ: Br. Med. J. (Online) **368**, m1165 (2020)
11. Day, M.: Covid-19: four fifths of cases are asymptomatic, China figures indicate. BMJ (Clin. Res. Ed.) **369**, m1375 (2020)
12. Li, R., Pei, S., Chen, B., Song, Y., Zhang, T., Yang, W., Shaman, J.: Substantial undocumented infection facilitates the rapid dissemination of novel coronavirus (SARS-CoV-2). Science **368**(6490), 489–493 (2020)
13. Nishiura, H., Kobayashi, T., Miyama, T., Suzuki, A., Jung, S., Hayashi, K., Kinoshita, R., Yang, Y., Yuan, B., Akhmetzhanov, A.R., et al.: Estimation of the asymptomatic ratio of novel coronavirus infections (COVID-19). Int. J. Infect. Dis. **94**, 154 (2020)
14. Mizumoto, K., Kagaya, K., Zarebski, A., Chowell, G.: Estimating the asymptomatic proportion of coronavirus disease 2019 (COVID-19) cases on board the Diamond Princess cruise ship, Yokohama, Japan, 2020. Eurosurveillance **25**(10), 2000180 (2020)
15. Dong, Y., Mo, X., Hu, Y., Qi, X., Jiang, F., Jiang, Z., Tong, S.: Epidemiological characteristics of 2143 pediatric patients with 2019 coronavirus disease in china. Pediatrics **16**(16), (2020)
16. Chen, Y., Wang, A., Yi, B., Ding, K., Wang, H., Wang, J., Xu, G.: The epidemiological characteristics of infection in close contacts of COVID-19 in Ningbo city. Chin. J. Epidemiol. **41**(5), 668–672 (2020)
17. Gao, Z., Xu, Y., Sun, C., Wang, X., Guo, Y., Qiu, S., Ma, K.: A systematic review of asymptomatic infections with COVID-19. J. Microbiol. Immunol. Infect. 1684–1182 (2020)
18. Bai, Y., Yao, L., Wei, T., Tian, F., Jin, D.-Y., Chen, L., Wang, M.: Presumed asymptomatic carrier transmission of COVID-19. JAMA **323**(14), 1406–1407 (2020)
19. Fraser, C., Riley, S., Anderson, R.M., Ferguson, N.M.: Factors that make an infectious disease outbreak controllable. Proc. Natl. Acad. Sci. **101**(16), 6146–6151 (2004)
20. Park, S.W., Cornforth, D.M., Dushoff, J., Weitz, J.S.: The time scale of asymptomatic transmission affects estimates of epidemic potential in the COVID-19 outbreak. Epidemics 100392 (2020)
21. McNeill, W.H., McNeill, W.: Plagues and Peoples. Anchor Books, New York (1998)
22. Bootsma, M.C.J., Ferguson, N.M.: The effect of public health measures on the 1918 influenza pandemic in us cities. Proc. Natl. Acad. Sci. **104**, 7588–7593 (2007)
23. Rubin, G.J., Amlôt, R., Page, L., Wessely, S.: Public perceptions, anxiety, and behaviour change in relation to the swine flu outbreak: cross sectional telephone survey. BMJ **339**, b2651 (2009)
24. Jones, J.H., Salathe, M.: Early assessment of anxiety and behavioral response to novel swine-origin influenza A (H1N1). PLoS ONE **4**(12), e8032 (2009)
25. Lau, J.T.F., Yang, X., Tsui, H.Y., Pang, E.: SARS related preventive and risk behaviours practised by Hong Kong-mainland China cross border travellers during the outbreak of the SARS epidemic in Hong Kong. J. Epidemiol. Community Health **58**(12), 988–996 (2004)
26. Gnanvi, J., Salako, K.V., Kotanmi, B., Kakaï, R.G.: On the reliability of predictions on Covid-19 dynamics: A systematic and critical review of modelling techniques. Infect. Disease Model. **6**, 258–272 (2021)
27. Wu, J.T., Leung, K., Leung, G.M.: Nowcasting and forecasting the potential domestic and international spread of the 2019-nCoV outbreak originating in Wuhan, China: a modelling study. Lancet **395**(10225), 689–697 (2020)
28. Mandal, M., Jana, S., Nandi, S.K., Khatua, A., Adak, S., Kar T.K.: A model based study on the dynamics of COVID-19: prediction and control. Chaos Solitons Fractals 109889 (2020)
29. Dobrovolny, H.M.: Modeling the role of asymptomatics in infection spread with application to SARS-CoV-2. PLoS ONE **15**(8), e0236976 (2020)
30. Funk, S., Salathé, M., Jansen, V.A.A.: Modelling the influence of human behaviour on the spread of infectious diseases: a review. J. R. Soc. Interface **7**(50), 1247–1256 (2010)
31. Bauch, C., d'Onofrio, A., Manfredi, P.: Behavioral epidemiology of infectious diseases: an overview. In Piero Manfredi and Alberto D'Onofrio, editors, Modeling the interplay between human behavior and the spread of infectious diseases, pp. 1–19. Springer, New York (2013)
32. Wang, Z., Bauch, C.T., Bhattacharyya, S., d'Onofrio, A., Manfredi, P., Perc, M., Perra, N., Salathé, M., Zhao, D. Stat. Phys. Vaccinat. Phys. Rep. **664**, 1–113 (2016)
33. Velasco-Hernández, J.X., Brauer, F., Castillo-Chavez, C.: Effects of treatment and prevalence-dependent recruitment on the dynamics of a fatal disease. Math. Med. Biol.: J. IMA **13**(3), 175–192 (1996)
34. Kribs-Zaleta, C.M.: Core recruitment effects in SIS models with constant total populations. Math. Biosci. **160**(2), 109–158 (1999)

35. Poletti, P., Caprile, B., Ajelli, M., Pugliese, A., Merler, S.: Spontaneous behavioural changes in response to epidemics. J. Theor. Biol. **260**(1), 31–40 (2009)
36. d'Onofrio, A., Manfredi, P., Salinelli, E.: Vaccinating behaviour, information, and the dynamics of SIR vaccine preventable diseases. Theor. Popul. Biol. **71**(3), 301–317 (2007)
37. d'Onofrio, A., Manfredi, P.: Information-related changes in contact patterns may trigger oscillations in the endemic prevalence of infectious diseases. J. Theor. Biol. **256**(3), 473–478 (2009)
38. Buonomo, B.: Effects of information-dependent vaccination behavior on coronavirus outbreak: insights from a SIRI model. Ricerche mat. **69**(2), 483–499 (2020)
39. Verelst, F., Willem, L., Beutels, P.: Behavioural change models for infectious disease transmission: a systematic review (2010–2015). J. R. Soc. Interface **13**(125), 20160820 (2016)
40. Del Valle, S.Y., Mniszewski, S.M., Hyman, J.M.: Modeling the impact of behavior changes on the spread of pandemic influenza. In: P. Manfredi and A. D'Onofrio (eds.) Modeling the Interplay Between Human Behavior and the Spread of Infectious Diseases, pp. 59–77. Springer, New York (2013)
41. Diekmann, O., Heesterbeek, J.A.P., Metz, J.A.J.: On the definition and the computation of the basic reproduction ratio R_0 in models for infectious diseases in heterogeneous populations. J. Math. Biol. **28**(4), 365–382 (1990)
42. Wu, Z., McGoogan, J.M.: Characteristics of and important lessons from the coronavirus disease 2019 (COVID-19) outbreak in China: summary of a report of 72314 cases from the Chinese Center for Disease Control and Prevention. JAMA **323**(13), 1239–1242 (2020)
43. Report of the WHO-China Joint Mission on Coronavirus Disease 2019 (COVID-19). https://www.who.int/docs/default-source/coronaviruse/who-china-joint-mission-on-covid-19-final-report.pdf. Published February 16, 2020. Access date: (2020)
44. Deng, Y., Liu, W., Liu, K., Fang, Y.-Y., Shang, J., Zhou, L., Wang, K., Leng, F., Wei, S., Chen, L., et al.: Clinical characteristics of fatal and recovered cases of coronavirus disease 2019 in Wuhan, China: a retrospective study. Chin. Med. J. **133**(11), 1261–1267 (2020)
45. Adhikari, S.P., Meng, S., Wu, Y.-J., Mao, Y.-P., Ye, R.-X., Wang, Q.-Z., Sun, C., Sylvia, S., Rozelle, S., Raat, H., et al.: Epidemiology, causes, clinical manifestation and diagnosis, prevention and control of coronavirus disease (COVID-19) during the early outbreak period: a scoping review. Infect. Dis. Poverty **9**(1), 1–12 (2020)
46. Bi, Q., Wu, Y., Mei, S., Ye, C., Zou, X., Zhang, Z., Liu, X., Wei, L., Truelove, S.A., Zhang, T., et al.: Epidemiology and transmission of COVID-19 in 391 cases and 1286 of their close contacts in Shenzhen, China: a retrospective cohort study. Lancet. Infect. Dis **20**(8), 911–919 (2020)
47. Wang, D., Bo, H., Chang, H., Zhu, F., Liu, X., Zhang, J., Wang, B., Xiang, H., Cheng, Z., Xiong, Y., et al.: Clinical characteristics of 138 hospitalized patients with 2019 novel coronavirus-infected pneumonia in Wuhan, China. JAMA **323**(11), 1061–1069 (2020)
48. Lan, L., Dan, X., Ye, G., Xia, C., Wang, S., Li, Y., Haibo, X.: Positive RT-PCR test results in patients recovered from COVID-19. JAMA **323**(15), 1502–1503 (2020)
49. Liu, Y., Gayle, A.A., Wilder-Smith, A., Rocklöv, J.: The reproductive number of COVID-19 is higher compared to SARS coronavirus. J. Travel Med. **27**(2), (2020)
50. Centers for Disease Control and Prevention. Interim Clinical Guidance for Management of Patients with Confirmed Coronavirus Disease (COVID-19). https://www.cdc.gov/coronavirus/2019-ncov/hcp/clinical-guidance-management-patients.html, Access date: (2021)